Fault Diagnosis in Stationary Rotor Systems through Correlation Analysis and Artificial Neural Network

Alexandre Carlos Eduardo[a] and Robson Pederiva[b]

[a]Federal University of Minas Gerais (UFMG).
Department of Mechanical Engineering (DEMEC)
aceduard@hotmail.com

[b]State University of Campinas (UNICAMP).
Faculty of Mechanical Engineering/Departament of Mechanical Design
robson@fem.unicamp.br

Abstract. *This work presents a methodology of parameters fault diagnosis in rotating mechanical systems excited by unbalance and coloured stochastic noise, through the correlation analysis based on the Ljapunov Matrix and the Artificial Neural Network (ANN). The procedure of parameter fault diagnosis described uses only measured state variables. The direct measurement of the stochastic excitation is not necessary. Coloured noise stochastic excitation is modeled using a dynamical system excited by white noise. The proposed method avoids the necessity of measuring the excitation forces and works on the displacement and velocity signals obtained form different points of the rotor system. Using correlation the output variables, it is possible to derive specific relations involving the physical parameters of the system and the correlation matrices of the measured variables. Faults in the rotor can be detected by monitoring the variation of the physical parameters through a comparison of theoretical and estimated correlation functions. Some variables are difficult to be measured and the correlation functions involving such variables cannot be directly estimated. Artificial Neural Network is used as a tool to map such correlations. The analysis of the results is made with the application of the method to a rotor system modeled with six degrees of freedom. The good results of these examples show the viability of further studies in this area.*

Keywords:*Fault Diagnosis, Correlations Analysis, Ljapunov Matrix Equation, Artificial Neural Network*

1. Introduction

Fault detection and diagnosis processes has been receiving considerable attention in recent years due to the obvious importance of this problem. In addition, the increasing availability of powerful computing environments and the progress in problem-solving paradigms has facilitated the application of a wide variety of methods for real-time diagnosis. Many of these methods were developed in different fields, such as in control theory, signal processing and artificial intelligence (AI). As a result, the methods differ with respect to the type of prior knowledge they are based on and how this knowledge is used for developing a diagnostic system.

At the heart of fault diagnosis lies the model-based approach, where by as many variables and system parameters are taken into account as possible, in order to construct a detailed mathematical model of the system under observation. Once the dynamic behaviour of the system has been "adequately" modelled, it should theoretically be possible to detect faults via analysis of changes in the model to input parameters. Several approaches are based on parity space equations, diagnostic observers, and process identification (Frank, 1990; Gertler, 1991; Patton and Chen, 1992; Isermann, 1984; Patton et al., 1989; Isermann, 1993, 1999; Chen et al., 1999). Venkatasubramanian et al (2003) conclude that these methods are based on the analytical redundancy inherent to modelling process. They also introduce the problem of fault diagnosis and review some approaches based on quantitative models.

Pederiva (1992) and Chiarello (1998) propose an alternative approach to face the problem of parameters estimation and fault detection in stationary dynamic systems. The relations between correlation functions and physical parameters are used and it is evidenc that the correlation functions tends to steady and constant values.

This work shows that it is possible to expand the proposed formulation by introducting the relations between the Ljapunov Matrix and the Artificial Neural Network (ANN). This procedure of parameter fault diagnosis uses only measured state variables. The correlation function involving only output variables can be estimated through the measurements of these variables. One can verify the compatibilty of the equation applying the estimated correlations in association with the theoretical values of the parameters. Equations that depend on parameters that have changed will present inconsistency and the others not. In this way, it is possible not only to detect changes in the system but also to locate them.

A numerical example shows that is also possible to locate the fault parameters, even when mechanical system are excited by stochastic forces.

2. Dynamical Model

Consider a rotor system that can be described by the following differential matrix equation,

$$M\ddot{\xi}(t) + P\dot{\xi}(t) + Q\xi(t) = Su(t) + Hn(t) \tag{1}$$

where the matrices *M*, *P* and *Q* are respectively, the mass, damping and stiffness matrices with appropriate dimensions. The matrices *S* and *H* are input matrices of stochastic forces, unbalance forces and harmonic perturbations. The vector ξ(t) is the *n* dimensional vector of displacements and the dots indicate differentiations with respect to time. The vector *u(t)* representing the stochastic forces is considered as a white noise process. It is easy to transform the above *n* dimensional equation into a *2n* dimensional state space model,

$$x^T(t) = \left\{\xi(t) \quad \vdots \quad \dot{\xi}(t)\right\}, \tag{2}$$

The state space equation can be obtained,

$$\dot{x}(t) = Ax(t) + Bu(t) + En(t) \tag{3}$$

with

$$A = \begin{bmatrix} 0 & I \\ -M^{-1}Q & -M^{-1}P \end{bmatrix} = \begin{bmatrix} 0_{(f,f)} & I_{(f,f)} \\ A_{1_{(f,f)}} & A_{2_{(f,f)}} \end{bmatrix} \tag{4}$$

$$B = \begin{bmatrix} 0 \\ M^{-1}S \end{bmatrix} = \begin{bmatrix} 0_{(f,p)} \\ B_{1_{(f,p)}} \end{bmatrix} \quad \text{and} \quad E = \begin{bmatrix} 0 \\ M^{-1}H \end{bmatrix} = \begin{bmatrix} 0_{(f,p)} \\ E_{1_{(f,p)}} \end{bmatrix} \tag{5}$$

The squared matrix *A* of order $n = 2f$ is called the system matrix; The matrix *B (n, p)* is the input matrix; and *n(t)* is a harmonic excitation given by,

$$n(t) = \begin{bmatrix} \cos(\Omega t) \\ sin(\Omega t) \end{bmatrix} \tag{6}$$

In Eq. (3), if *u(t)* is not a white noise it may be modelled as the output of a similar dynamic system (filter). Considering the dynamic system

$$\dot{z}(t) = Rz(t) + S^* w(t) \tag{7}$$

$z(t)$ is the state vector *t*-dimensional.

The input *u(t)* of in dynamic equation (3) is a coloured process,

$$u(t) = H_u z(t) \tag{8}$$

H_u is a matrix with dimension *(p,t)*.

Figure 1 shows the diagram of a dynamic system excited by coloured noise

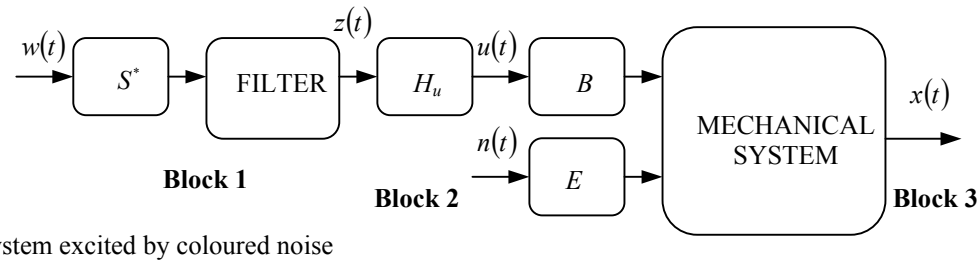

Figure 1 – Dynamic system excited by coloured noise

The figure 1 shows blocks the dynamic system excited by coloured noise, where: Block 1- modeling coulored noise through white noise; Block 2- composition of excitation modeled as the output of a similar dynamic system (filter); Block 3- response of system mechanical.

An expanded model is then obtained as a result of the composition of the system equation and the filter equation. This new expanded showed in Fig. (1), is similar to Eq. (3), with new matrices A^* and B^*, Eq. (9).

Associating equations (7), (8) and (3) one can obtain the expanded dynamic equation

$$\dot{x}^*(t) = A^* x^*(t) + B^* w(t) + E^* n(t) \tag{9}$$

with,

$$\cdot x^*(t) = \begin{Bmatrix} x(t) \\ \cdots \\ z(t) \end{Bmatrix} \tag{10}$$

$$B^* = \begin{Bmatrix} 0_{(12,1)} \\ \cdots \\ s_1 \\ s_2 \end{Bmatrix} \text{ and } E^* = \begin{Bmatrix} E_{(12,2)} \\ \cdots \\ 0_{(2,2)} \end{Bmatrix} \tag{11}$$

The new matrix of the system A^* has the following structure

$$A^* = \begin{bmatrix} A & \vdots & B \\ \cdots & \vdots & \cdots \\ 0 & \vdots & R \end{bmatrix} \tag{12}$$

2.1 Physical Model

The mechanical system considered is a rotor with a flexible shaft coupled to a fixed end eletric motor. Between the motor and the disc, there is a bearing of mass m_1 fixed elastically. The six degrees of freedom are the four translations and two rotations ilustrated in the Figure 2. Table (1) shows the numerical values used in the simulations.

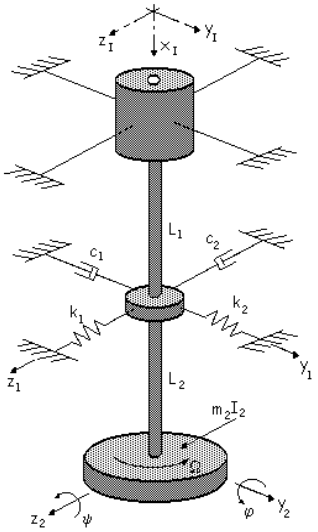

Table 1: Values parameters

Parameters	Values	Unit
m_1	15	kg
m_2	10	kg
I_2	0.25	$kg.m^2$
I_{2polar}	0.50	$kg.m^2$
L_1=L_2	0.4	m
k_1	90.000	N/m
k_2	120.000	N/m
c_1	30.000	kg/s
c_2	37.500	kg/s
Ω	60	rad/s

Figure 2- The 6-DOF model

The displacements are represented in the vectors,

$$\xi^T = \{y_1 \quad y_2 \quad \psi \quad z_1 \quad z_2 \quad \varphi\} \tag{13}$$

The diagonal mass matrix *M* is,

$$M = diag\{m_1 \quad m_2 \quad I_2 \quad m_1 \quad m_2 \quad I_2\} \tag{14}$$

The matrix S has the following structure,

$$S^T = \{s_1 \quad s_2 \quad s_3 \quad s_4 \quad s_5 \quad s_6\}, \tag{15}$$

with s_i (i=1,...6) constants values. The matrix H is,

$$H = \begin{bmatrix} 0 & 0 \\ m_2 e\Omega^2 & 0 \\ 0 & 0 \\ \dots & \dots \\ 0 & 0 \\ 0 & m_2 e\Omega^2 \\ 0 & 0 \end{bmatrix}, \tag{16}$$

where e is the rotor unbalance eccentricity.

2.2 Response of Dynamical System Excited by Coloured Noise

The time response of the linear system is a superposition of the response due to the stochastic excitation $x_w(t)$ and the response caused by unbalance $x_n(t)$,

$$x^*(t) = x_w(t) + x_n(t) = x_w(t) + q_1 \cos\Omega t + q_2 sin\Omega t \tag{17}$$

with q_1 and q_2 representing n–dimensional amplitudes vectors. The correlation matrix, $R_{x^*x^*}(\tau_i)$ can be defined as Yaglom (1962),

$$R_{x^*x^*}(\tau_i) = \varepsilon\left\{x^*(t).x^{*T}(t+\tau_i)\right\} \tag{18}$$

where τ_i represents a time lag. Substituting the solution of the state space, Eq.(9), and with Eq.(17) into Eq. (18), the following relation can be obtained for stationary condition (Yaglom, 1962),

$$A^* R_{x^*x^*}(\tau_i) + R_{x^*x^*}(\tau_i)A^{*T} + E^* R_{nx^*}(\tau_i) + R_{x^*n}(\tau_i)E^{*T} = -B^* \psi_{ww} B^{*T} e^{A^{*T}\tau_i}, \tag{19}$$

where the matrix ψ_{ww} is the intensity matrix of the excitation process w(t). The eq. (19) is called Ljapunov Matrix Equation be used to develop the method of fault detection described in this work. Expanding the Eq. (19),

$$\begin{bmatrix} 0 & I & 0 \\ A_1 & A_2 & B \\ 0 & 0 & R \end{bmatrix}\begin{bmatrix} R_{\xi\xi} & R_{\xi\dot{\xi}} & R_{z\dot{\xi}} \\ R_{\dot{\xi}\xi} & R_{\dot{\xi}\dot{\xi}} & R_{\dot{\xi}z} \\ R_{\dot{\xi}z} & R_{z\xi} & R_{zz} \end{bmatrix} + \begin{bmatrix} R_{\xi\xi} & R_{\xi\dot{\xi}} & R_{z\dot{\xi}} \\ R_{\dot{\xi}\xi} & R_{\dot{\xi}\dot{\xi}} & R_{\dot{\xi}z} \\ R_{\dot{\xi}z} & R_{z\xi} & R_{zz} \end{bmatrix}\begin{bmatrix} 0 & A_1^T & 0 \\ I & A_2^T & 0 \\ 0 & B^T & R^T \end{bmatrix} +$$
$$\begin{bmatrix} 0 \\ E_1 \\ 0 \end{bmatrix}\begin{bmatrix} R_{n\xi} & R_{n\dot{\xi}} & R_{nz} \end{bmatrix} + \begin{bmatrix} R_{n\xi} \\ R_{n\dot{\xi}} \\ R_{nz} \end{bmatrix}\begin{bmatrix} 0 & E_1^T & 0 \end{bmatrix} = -\begin{bmatrix} 0 & 0 & 0 \\ 0 & 0 & 0 \\ 0 & 0 & B_1 \psi_{ww} B_1^T \end{bmatrix} e^{A^T \tau_1} \tag{20}$$

The sub matrices multiplications of the Eq. (20) provide the following equation ,

$$R_{\dot{\xi}\dot{\xi}}(\tau_i) + R_{\xi\xi}(\tau_i)A_1^T + R_{\xi\dot{\xi}}(\tau_i)A_2^T + R_{z\dot{\xi}}(\tau_i)B^T + R_{n\xi}E_1^T = 0 \tag{21}$$

Equation (21) is n-dimensional and contain the relations between the correlation functions of the output (displacements and velocities) and the physical parameters Eq. (1). Equation (21) contains also the correlation between the unbalance forces and the output. Althought, it can be further developed and simplified.

The correlation matrix between unbalance and output variables can be evaluate. From the definition

$$R_{nx^*}(\tau_i) = \varepsilon\left\{n(t).x^{*T}(t+\tau_i)\right\} \tag{22}$$

$$R_{x^*n}(\tau_i) = \varepsilon\{x^*(t).n^T(t+\tau_i)\} \tag{23}$$

Substituting the equations (6) and (17) in to (22) and (23) ,and after some mathematical manupulation we obtain,

$$R_{x^*n}(\tau_i) = \frac{1}{2}\cos\Omega\tau_i(q_1+q_2)+\frac{1}{2}sin\Omega\tau_i(q_1-q_2) \tag{24}$$

$$R_{nx^*}(\tau_i) = \frac{1}{2}\cos\Omega\tau_i(q_1^T+q_2^T)+\frac{1}{2}sin\Omega\tau_i(q_2^T-q_1^T) \tag{25}$$

It means that under stationary condition the numeric values of matrices R_{x^*n} and R_{nx^*} are constants depending on the amplitudes q_1 and q_2, the rotation speed and the time lag (τ_i). The terms containing this correlations in the Eq.(21) are constants too. Equation (21) represents the base for the proposed approach and contains relations of compatibility. On can verify some variation on the parameters by checking these relations.

The matrices A_1 and A_2 in the Eq.(21) have the following internal structure (Pederiva, 1992),

$$A_1^T = \begin{bmatrix} k_{11} & k_{12} & k_{13} & 0 & 0 & 0 \\ -k_{22} & k_{22} & k_{23} & 0 & 0 & 0 \\ -k_{32} & k_{32} & k_{33} & 0 & 0 & 0 \\ 0 & 0 & 0 & k_{44} & k_{12} & -k_{13} \\ 0 & 0 & 0 & -k_{22} & k_{22} & -k_{23} \\ 0 & 0 & 0 & k_{32} & -k_{32} & k_{33} \end{bmatrix} \tag{26}$$

$$A_2^T = \begin{bmatrix} c_{11} & 0 & 0 & 0 & 0 & 0 \\ 0 & 0 & 0 & 0 & 0 & 0 \\ 0 & 0 & 0 & 0 & 0 & -\Omega I_{2p} \\ 0 & 0 & 0 & c_{44} & 0 & 0 \\ 0 & 0 & 0 & 0 & 0 & 0 \\ 0 & 0 & \Omega I_{2p} & 0 & 0 & 0 \end{bmatrix} \tag{27}$$

Expanding Eq.(21) on can obtain the following relations involving the parameters of the bearing, the shaft and the unbalance:

$$R_{\xi\dot{\xi}_{77}} + R_{\xi\xi_{11}} * k_{11} + R_{\xi\xi_{12}} * k_{12} + R_{\xi\xi_{13}} * k_{13} + R_{\xi\xi_{17}} * c_{11} + R_{\xi_{11}} * b_1 = 0 \tag{28}$$

$$R_{\xi\dot{\xi}_{78}} + R_{\xi\xi_{11}} * k_{22} + R_{\xi\xi_{12}} * k_{22} + R_{\xi\xi_{13}} * k_{23} + R_{\xi\eta} * e\Omega^2 = 0 \tag{29}$$

$$R_{\xi\dot{\xi}_{79}} + R_{\xi\xi_{11}} * k_{32} + R_{\xi\xi_{21}} * k_{13} + R_{\xi\xi_{13}} * k_{33} + R_{\xi\xi_{23}} * k_{23} + R_{z\xi} * b_3 = 0 \tag{30}$$

$$R_{\xi\dot{\xi}_{710}} + R_{\xi\xi_{14}} * k_{44} + R_{\xi\xi_{15}} * k_{12} - R_{\xi\xi_{16}} * k_{13} + R_{\xi\xi_{110}} * c_{44} = 0 \tag{31}$$

The indices in $R_{\xi\xi ij}$ indicate the correlation between the state variable i and the state variable j. The equations of compatibility (28) to (31) have different dependences on the parameters. For example, in the Eq.(28) only three parameters appear. It means that this equation is not sensitive to the parameter *e* related to the unbalance. It is also insensitive to parameters k_{44} and k_{33}. This property is very useful, not only to determine variations in the parameters but also to locate where the failure is present.

3. Proposed Method

It is proposed a methodology for fault diagnosis in stationary rotor systems through correlation analysis and artificial neural network using multi-layer perceptron to map the correlation functions involving variables that cannot be directly estimated. Multi-layer perceptrons (MLP) are neural nets usually referred to as function approximators. A MLP is a generalization of Rosenblatt's perceptron (1958).The fundamental importance of a neural network is not only the way a neuron is implemented but also how their interconnections (more commonly called topology) are made.

One of the easiest forms of this topology in recent years is made of three layers :

- one input layer (the inputs of the network)
- one hidden layer
- one output layer (the outputs of the network)

All neurons from one layer are connected to all neurons in the next layer. One way to do this is by representing the mapping of equations (28) to (31), as illustrated in the Fig. 3. Applying estimated correlation functions on the input and comparing the output, in this case, the correlation function $R_{\dot{\xi}\dot{\xi}_{77}}$.

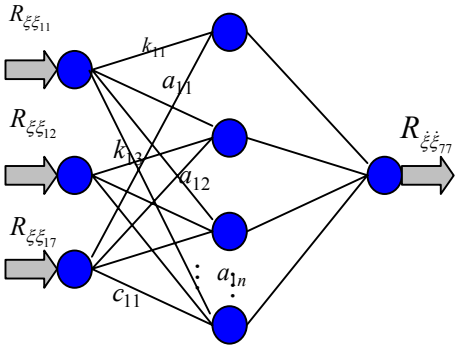

Figure 3- The structure neural for equation (28)

Each input has an associated weight W_{in}. The unit computes some function f of the weighted sum of its inputs:

$$R_{\dot{\xi}\dot{\xi}_{77}} = f\left(\sum_{i=1}^{n} R_{in} W_{in}\right) \tag{32}$$

- The weighted sum $\sum_{n} R_{in} w_{in}$ is called the net input to unit *i*, often written net_i.
- Note that W_{in} refers to the weight from unit *n* to unit *i*.
- The function *f* is the unit's activation function. In the simplest case, *f* is the identity function, and the unit's output is just its net input. This is called a linear unit.

Structurally, this net is composed by three neurons in input layer (corresponding the correlations functions), fifteen neurons in layer hidden (physical parameters of the system $c_{11} \ldots k_{11}$ and random weights $a_{11} \ldots a_{1n}$) and an output layer (corresponding the correlation function associated with the velocity vector). The correlations associated to the rotations and velocities coordenates of the rotor had been disconsidered (Eqs. 28 to 31). It is effect was trained by the net. For the architecture 1 of the neural net it was used the functions $R_{\xi\xi_{11}}$, $R_{\xi\xi_{12}}$ and $R_{\xi\xi_{17}}$ at the input layer and $R_{\dot{\xi}\dot{\xi}_{77}}$ at the output layer. For the architecture 2 of the neural net it was used the functions $R_{\xi\xi_{11}}$, $R_{\xi\xi_{12}}$ and $R_{\xi n}$ at the input layer and $R_{\dot{\xi}\dot{\xi}_{78}}$ at the output layer. For the architecture 3 of the neural net it was used the functions $R_{\xi\xi_{11}}$ and $R_{\xi\xi_{21}}$ at the input layer and $R_{\dot{\xi}\dot{\xi}_{79}}$ at the output layer. For the architecture 4 of the neural net it was used the functions $R_{\xi\xi_{14}}$, $R_{\xi\xi_{15}}$ and $R_{\xi\xi_{110}}$ at the input layer and $R_{\dot{\xi}\dot{\xi}_{710}}$ at the output layer.

4. Results

In order to demonstrate the applicability of the proposed approach, some operational situations of the dynamic behaviour a rotating system had been simulated.

The response of dynamical system excited by coloured noise was analyzed for different cut frequencies. The Figure 4 shows to the distribution of the coloured noise-type excitation generated from the white noise. The study of the variations of the parameters with the cutoff-frequency is associate to parameters variations in the resonance region.

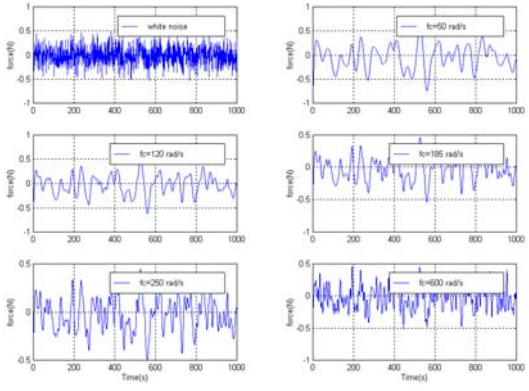

Figure 4- Distribution of the excitations coloured noise

To simulate a failure, the value of the parameter was changed about 20%. The system was simulated and the correlations calculated and the neural nets as described was trained. The output of the net from the fault condition was compared to one without failure. To compare the outputs it was used a Mean Squared Deviation (MSD) between the functions.

4.2 Studies cases

Equations (28 to 31) represent the base for the proposed approach and it contains relations of compatibility. One can verify some variation on the parameters by checking these relations. Table 2 shows the subjective percentage of fault

Table 2: Values parameters

Fault conditions	Fault Description
1	reduction of 20% k_{11}
2	reduction of 20% c_{11}
3	reduction of 20% c_{44}
4	reduction of 20% unbalanced
5	reduction of 20% k_{11} and k_{44}
6	reduction of 20% c_{11} and c_{44}
7	reduction of 20% k_{11} and unbalanced
8	reduction of 20% unbalanced and c_{44}

4.2.1 Variations in the parameters of the system and cutoff frequencies of the filter

Figures 5(a)-(d) show the deviations of the four equation considered (28) to (31). It is considered variations in cut-off frequencies for the fault conditions 1 to 4(table 2)

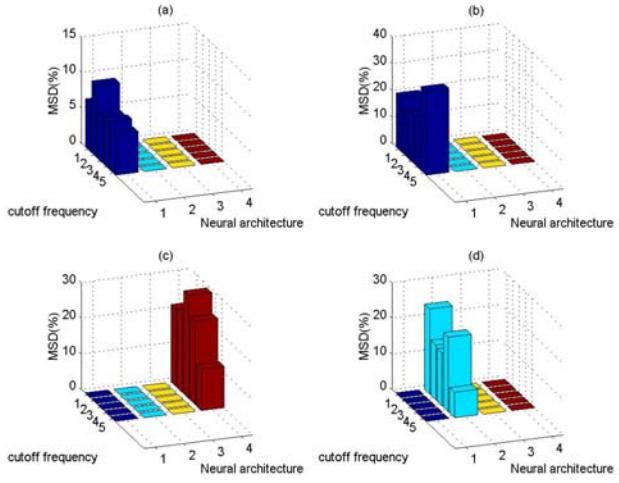

Figure 5 (a)-(d) - Squared Mean Deviation of network output: parameters variations and cutoff frequency.

Figure 5(a) shows the effect of the variation in the parameter k_{11}. It is observed that for different cutoff frequencies of the filter, the neural architecture 1 approximately presents variation. This fact is not found in the other architectures (equations 29 to 31). It means that are not dependent on the parameter k_{11}. Figure 5(b) shows the behavior of the architecture associated with a variation in the parameter c_{11}. It is interesting to note that the Eq.(28) presents a significant variation when compared to the behavior of the other equations. This is because equations (29) to (31) are not dependent on the parameter. c_{11} Figure 5(c) shows the behavior of the equations associated with a variation in the parameter c_{44}. The same behavior occurs, indicating that the failure is associated with Eq.(31). One can see that the equation associated with this parameter presents a great variation when compared to the others, indicating that the

failure is associated to the parameters of this equation. Finally, Fig. 5(d) ilustrates the variation in the unbalance of the rotor. The conclusions are similar to the cases already commented.

These cutoff frequency showed in Fig.4 (a)-(d) are distribution of the excitations coloured noise (Fig. 4).

Table 3 shows this correspondency. The Table 4 shows the correspondency neural architecture.

Table 3: Correspondency cuttoff frequency

axis y	Cutoff frequency
1	f_c= 50 rad/s
2	f_c= 120 rad/s
3	f_c= 185 rad/s
4	f_c= 250 rad/s
5	f_c= 600 rad/s

Table 4: Correspondency Neural architecture

axis x	Neural architecture
1	Eq. 28
2	Eq. 29
3	Eq. 30
4	Eq. 31

4.2.2 Combining Variations in the parameters and cutoff frequencies

Figures 6(a)-(d) show the deviations of the four equation considered (28) to (31). It considered different cut-off frequencies for the fault conditions 5 to 8(table 2).

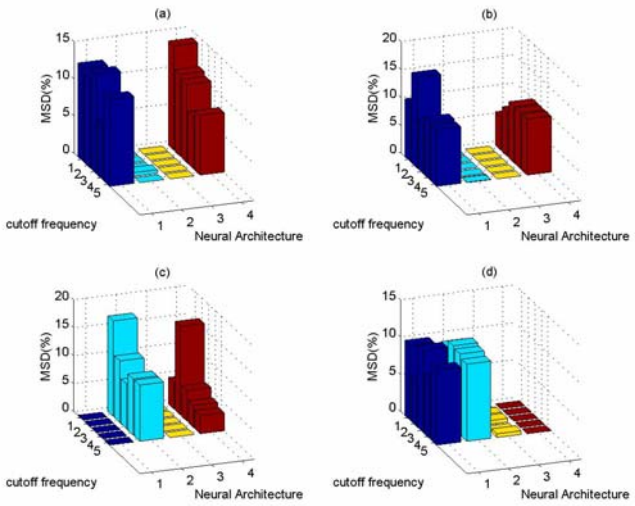

Figure 6(a)-(d) - Squared Mean Deviation of network output: parameters variations and cutoff frequency

Figure 6(a) shows the behavior of the architecture associated with a variation in the parameter c_{11} and c_{44}. It is interesting to note that equations (28) and (31) presents a significant variation when compared to the behavior of the other equations. Figure 6(b) shows the behavior of the architecture associated with a variation in the parameters k_{11} and k_{44}. The conclusions are similar to the cases already commented. Figure 6(c) shows the behavior of the architecture associated with a variation in the parameters unbalance and c_{44}. The equations (29) and (31) presents a significant variation when compared to the behavior of the other equations. Finally, Fig. 6(d) shows the variation in the unbalance of the rotor and the parameter c_{11} .Here the same behavior occurs, indicating that the failure is associated with equations (28 and 29). One can see that the equation associated with this parameter presents a great variation when compared to the others, indicating that the failure is associated with the parameters of this equation.

4.2.3 Percentuals Variations of coloured noise in system output

Figure 7(a)-(d) show the deviations of the four equations considered, Eqs. (28) to (31). The parameters are considered to be constants. Coloured noise is additioned in system output (variations in the order of 1 up to 5% of value RMS of the original signal).

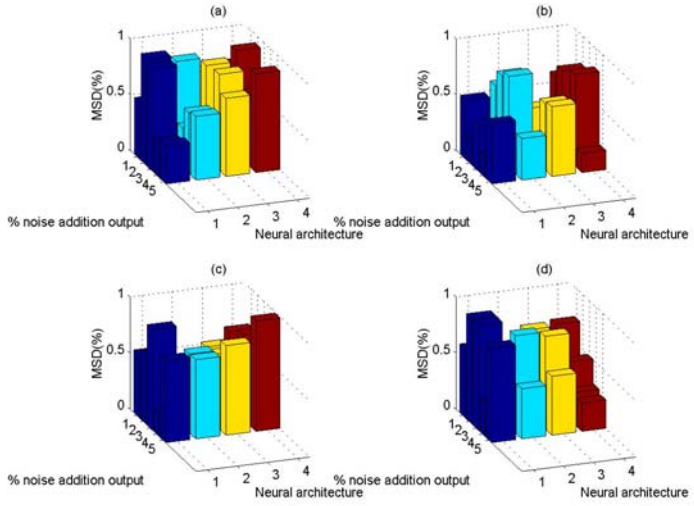

Figure 7(a)-(d) - Squared Mean Deviation of network output: variations of coloured noise output

One can see that the equations (28) to (31) do not present a great parameter variation, indicating that the failure is associated with the coloured noise added in system output of theses equations. In addition, the effect of coloured noise is minimized at the outputs of the nets for different architectures and noise levels.

5. Conclusions

In this work, a method of fault monitoring of a rotating system was developed, using the association of Ljapunov Matrix Equation and artificial neural network. The model simulated for the studied cases presented satisfactory results. In the considered method, there is no necessity to know the excitation force. However, the knowledge of the type and the form of the excitation is necessary. It is possible for a certain operational condition of the rotating mechanicalal system, to identify and to locate the fault exactly.

6. Acknowledgement

The authors would like to thank CNPq (Process 140613/1999-4*)* for financial support.

7. References

Chen, J. and Patton, R. J., 1999. Robust Model-Based Fault Diagnosis for Dynamic Systems. Kluwer Academic Publisher.

Chiarello, G.A.,1998. Fault Detection in Mechanical Systems through Correlation Analysis. PhD thesis, State University of Campinas (UNICAMP).

Frank, P. M. 1990. Fault Diagnosis in Dynamic Systems using Analytical and Knowledge-Based Redundancy - A Survey and Some New Results. Automatica, vol.26, no 3, pp.459- 474.

Gertler, J. 1991. Analytical Redundancy Methods in Fault Detection and Isolation - A Survey and Synthesis. In: Plenary paper, IFAC Safeprocess Symposium, Baden-Baden, Germany, sep. 10-13.

Isermann, R. 1984. Process Fault Detection based on Modeling and Estimation Methods - A survey. Automatica, pp.387-404, vol.20, n 4.

Isermann, 1993. R. Fault Diagnosis of Machines via Parameter Estimation and Knowledge Processing - Tutorial paper. Automatica, vol.29, n4, pp. 815-835.

Patton, R.J., Frank, P. and Clark, R.,1989. Fault Diagnosis in Dynamic Systems, Prentice Hall, UK.

Patton, R., J., Chen, J. 1992. On-line Residual compensation in Robust Fault Diagnosis of Dynamic Systems. In: IFAC Artificial Intelligence in Real Time Control, Delft, The Netherland. Proceedings, pp.221-227.

Pederiva, R. 1992. Parameter Identification of Mechanical Systems excited by Stochastic Forces. PhD. Thesis, State University of Campinas (UNICAMP).

Rosenblatt, F., 1958. The Perceptron: A Probabilistic Model for Information Storage and Organization in the Brain. Psychological Review, 65, 386-408.

Venkatasubramanian V., Rengaswamy R. , Yin, K. , Kavuri, S.N., 2003. A Review of Process Fault Detection and Diagnosis Part I: Quantitative Model-based Methods Computers and Chemical Engineering 27 pp. 293-311.

Yaglom, A. M. 1962. An Introduction to the Theory of Stationary Random Functions, Prentice Hall, 1962.